TISSUE ENGINEERING: Part A
Volume 18, Numbers 23 and 24, 2012

DOI: 10.1089/ten.tea.2011.0711

Hyaluronic Acid-Binding Scaffold for Articular Cartilage Repair

Shimon A. Unterman, Ph.D.,[1,2] Matthew Gibson, B.S.,[1,2] Janice H. Lee, Ph.D.,[1,2] Joshua Crist, M.S.,[1,2] Thanissara Chansakul, B.S.,[1,2] Elaine C. Yang, B.S.,[1,2] and Jennifer H. Elisseeff, Ph.D.[1,2]

Hyaluronic acid (HA) is an extracellular matrix molecule with multiple physical and biological functions found in many tissues, including cartilage. HA has been incorporated in a number of biomaterial and scaffold systems. However, HA in the material may be difficult to control if it is not chemically modified and chemical modification of HA may negatively impact biological function. In this study, we developed a poly(ethylene glycol) hydrogel with noncovalent HA-binding capabilities and evaluated its ability to support cartilage formation *in vitro* and in an articular defect model. Chondrogenic differentiation of mesenchymal stem cells encapsulated in the HA-interactive scaffolds containing various amounts of exogenous HA was evaluated. The HA-binding hydrogel without exogenous HA produced the best cartilage as determined by biochemical content (glysocaminoglycan and collagen), histology (Safranin O and type II collagen staining), and gene expression analysis for *aggrecan, type I collagen, type II collagen,* and *sox-9*. This HA-binding formulation was then translated to an osteochondral defect model in the rat knee. After 6 weeks, histological analysis demonstrated improved cartilage tissue production in defects treated with the HA-interactive hydrogel compared to noninteractive control scaffolds and untreated defects. In addition to the tissue repair in the defect space, the Safranin O staining in cartilage tissue surrounding the defect was greater in treatment groups where the HA-binding scaffold was applied. In sum, incorporation of a noncovalent HA-binding functionality into biomaterials provides an ability to interact with local or exogenous HA, which can then impact tissue remodeling and ultimately new tissue production.

Introduction

Hyaluronic acid (HA) is used extensively in tissue engineering scaffolds due to its important structural and signaling roles in a variety of tissues, including the joint. It is a nonsulfated glysocaminoglycan (GAG) composed of repeating disaccharide units of glucuronic acid and N-acetylglucosamine. The carboxylate group of glucuronic acid allows for relatively facile crosslinking and chemical modification of HA to form hydrogels or sponges, which has led to its evaluation as a scaffold material for a variety of tissues.[1–7] However, the resultant HA-based scaffolds exhibit little similarity with the natural structure and presentation of HA found in the body. The bioactivity of HA is highly dependent on the molecular weight of the polymer and its associations with other proteins and extracellular matrix (ECM) components, and it is unclear how crosslinked HA scaffolds would affect cellular behavior compared to its natural presentation. Furthermore, the covalent modification of the HA backbone itself may significantly change its biological activity in unanticipated ways. A more natural, biologically relevant presentation of the HA may yield greater insight into the effects of HA-based scaffolds for tissue engineering, and may better potentiate tissue repair.

Cartilage tissue engineering aims to develop an effective therapy to repair articular cartilage lost due to trauma or disease. Cartilage has poor endogenous repair capacity, and currently available therapies are largely ineffective at producing a robust, healthy repair tissue. Given the aging population and increasing incidence of cartilage damage and osteoarthritis, there is significant interest in cartilage repair and restoring joint function. Biomaterials play an important role in serving as a scaffold to direct tissue repair. Tissue engineering scaffolds normally are composed of combinations of biological and synthetic polymer systems. While biological polymer systems often exhibit good bioactivity and regeneration potential, they frequently are mechanically weak, and difficult to control and purify. Attempts to chemically modify biological polymers to increase scaffold strength and control are often challenging and may cause a

[1]Translational Tissue Engineering Center, Wilmer Eye Institute, Johns Hopkins University, Baltimore, Maryland.
[2]Department of Biomedical Engineering, Johns Hopkins University, Baltimore, Maryland.

loss of biological activity.[8] In contrast, synthetic systems boast a high degree of control over physical properties, but exhibit little to no biological activity.[9,10] Of recent interest is the combination of synthetic materials with biologically active molecules to form biosynthetic composite materials that share the high degree of control found in synthetic materials with the biological functionalities found in biological polymers. These composite biomaterials include synthetic polymers modified with bioactive proteins or peptides to introduce specific biological functionalities such as cell adhesion, growth factor activity, or cell-mediated degradation.[11] Short, synthetic peptides are easy to synthesize, purify, and modify, yet still exhibit significant biological activity. IKVAV, YRGDS, collagen mimetic peptides, and matrix metalloproteinase-sensitive peptides are all examples of peptides that have been incorporated into biomaterial systems to introduce biological functionalities.[11–14] More recently, scaffolds that were engineered with fibronectin domains designed to simultaneously interact with growth factors as well as integrins were shown to enhance growth factor-driven wound healing through local presentation of growth factors to cells.[15] These techniques allow for the controlled introduction of specific biological functionalities to a broader polymer system to tailor the cellular microenvironment for the desired task.

To achieve a more natural presentation of HA, we designed an HA-interacting hydrogel scaffold that noncovalently binds HA. Mummert *et al.* discovered an HA-binding peptide (HABPep) through phage display that specifically binds HA that was applied to inhibiting HA-mediated leukocyte trafficking. Moreover, a fluorescent-labeled derivative of HABPep can efficiently and specifically label HA in tissues.[16,17] In this study, we conjugated HABPep to a synthetic hydrogel scaffold based on poly(ethylene glycol) diacrylate (PEGDA) and investigated the resulting biomaterial's ability to interact with HA using an *in vitro* model system. This scaffold can interact with HA in the local ECM environment, including cell-secreted HA and exogenously supplied HA. We hypothesized that this HA-interacting hydrogel would improve chondrogenesis of bone marrow-derived mesenchymal stem cells (MSCs) in an *in vitro* culture system, since HA is a key molecule in cartilage matrix. To extend this to a clinically relevant model, we implanted the HABPep-functionalized hydrogels in a rat osteochondral defect model to determine their ability to potentiate cartilage repair *in vivo*.

Materials and Methods

Synthesis of HA binding-hydrogels

HA-binding peptide (HABPep; sequence GAHWQFNALTVR) and sequence-scrambled HABPep controls (sHABPep; WRHGFALTAVNQ) were synthesized using standard Fmoc-mediated solid-phase peptide synthesis on a Symphony Quartet peptide synthesizer (Protein Technologies). Following synthesis, peptides were cleaved using a solution of trifluoroacetic acid, triisopropylsilane, and water in a 95:2.5:2.5 ratio. The crude product was purified using reverse-phase high-performance liquid chromatography (HPLC, C18 Grace-Vydac column) on a water/acetonitrile gradient. Purified peptides were frozen and lyophilized; identity of purified peptides was confirmed using matrix-assisted laser-desorption ionization time of flight (MALDI-TOF) mass spectroscopy (Voyager DE-STR; Applied Biosystems).

Peptides were conjugated to acryl-PEG-N-hydroxysuccinimide (Acryl-PEG-NHS; 3.4 kD, Laysan Bio) as previously described.[11] Briefly, peptides were reacted with a 1.2-fold molar excess of PEG in 50 mM sodium bicarbonate at pH 8.0 for 2 h at room temperature. The resultant acryl-PEG-peptides were lyophilized and stored at −20°C.

HA-interacting scaffolds were prepared by dissolving 10% (w/v) polyethylene glycol diacrylate (PEGDA; 3.4 kD, Sunbio) with 2% (w/v) acryl-PEG-HABPep and 0.05% photoinitiator (Irgacure 2959; Ciba) in phosphate-buffered saline (PBS; Invitrogen). Controls without HA-binding functionality were substituted with either sequence-scrambled 2% acryl-PEG-sHABPep or 2% PEG monoacrylate (PEGMA; 5 kD, Laysan Bio in place of HABPep). Macromers were combined with HA solutions as indicated (HA; 980 kD, Lifecore). Cylindrical polypropylene molds (~5.5-mm diameter) were filled with 100 μL of macromer solution. The solution was polymerized by exposure to ultraviolet light at 365 nm (5 mW/cm^2) for 5 min.

Quantification of HA release from hydrogels

Release of HA from hydrogels was determined as a function of HA loading and presence of HABPep. Control sHABPep hydrogels were prepared with 0, 1, 5, 10, and 20 mg/mL HA. HABPep scaffolds were prepared with 5 mg/mL HA, based on preliminary studies indicating that concentration had little nonspecific interactions between the HA and the PEG network. Polymerized constructs were immersed in PBS or 50 U/mL hyaluronidase solution (Sigma), which were collected at various time points and assayed for the presence of HA using a carbazole assay as previously shown.[18] Briefly, 3 mL sodium tetraborohydrate solution (9.5 mg/mL in sulfuric acid, Sigma) was placed in test tubes and cooled to 4°C. Glucuronic acid standards or samples (0.5 mL) were carefully layered over the sodium tetraborohydrate. Tubes were then heated for 10 min in a boiling water bath and cooled to room temperature. Carbazole solution (0.1/mL, 12.5/mg in 9.9875/g of ethanol, Sigma) was added to the tubes and shaken. The test tubes were heated in a boiling water bath for 15 min and cooled to room temperature. Absorption of the samples was measured at 530 nm against water blanks and compared to a glucuronic acid standard curve. All experiments were performed in triplicate.

Chondrogenic differentiation of goat MSCs

Goat bone marrow-derived MSCs were isolated and expanded as previously described.[19] After three or four passages, MSCs were trypsinized, centrifuged, and resuspended in a macromer solution containing 10% PEGDA and 2% acryl-PEG-peptide or PEGMA as well as varying HA concentrations (0, 0.5, 2.5, 5 mg/mL). Cells were suspended at 20 million/mL and hydrogels polymerized in 100-μL cylindrical molds as described above. Hydrogel constructs were transferred to 24-well plates containing the chondrogenic differentiation medium containing 100 nM dexamethasone (Sigma), 40 mg/L Proline (Sigma), 50 mg/L ascorbic acid-2-phosphate (Sigma), 100 mg/L sodium pyruvate (Invitrogen), 50 mg/mL ITS Premix (insulin, transferring, selenous acid; BD Biosciences), 1% penicillin/streptomycin (Invitrogen), and 10 ng/mL transforming growth factor β (TGFβ-1).

Constructs were cultured for up to 6 weeks, after which they were evaluated on the basis of biochemical content, chondrogenic gene expression, and histological analysis.

Biochemical characterization of in vitro *chondrogenesis*

Hydrogel constructs were harvested at time points up to 6 weeks for biochemical analysis as previously described.[19] Constructs were weighed, lyophilized, and weighed again to obtain a dry weight and a swelling ratio. Dried hydrogels were homogenized with pellet pestles and digested overnight in papain (Worthington Biochemical). DNA content was assayed using Hoescht 33258 dye (Molecular Probes) and a DynaQuant 200 fluorometer (Hoefer) against a calf thymus DNA standard curve. Glycosaminoglycan (GAG) content was assayed by measuring absorbance at 525 nm with dimethylmethylene blue dye against a standard curve using chondrotin sulfate C (Sigma). A hydroxyproline assay was used to determine collagen content by hydrolysis overnight in hydrochloric acid followed by reaction with p-dimethylaminobenzaldehyde (Sigma) and chloramine T (Sigma). Absorbance was read on a spectrophotometer at 563 nm and compared to hydroxyproline standards (Sigma). Biochemical content was normalized to DNA content and dry weight to account for variations in the construct size and cellularity. All biochemical data had a sample size of 4.

Histological characterization of in vitro *chondrogenesis*

Hydrogel constructs were fixed in 4% paraformaldehyde (Sigma) and stored in 70% ethanol. Constructs were dehydrated, embedded in paraffin, and sectioned into 5-μm sections using a microtome (Leica). Sections were stained with Safranin O to assess GAG content. Immunohistochemistry was performed using rabbit polyclonal antibodies against type I and type II collagen followed by visualization with horseradish peroxidase using the Histostain SP kit (Invitrogen). Images were captured using a Zeiss Axiovert microscope.

Real-time polymerase chain reaction analysis of in vitro *chondrogenesis*

Constructs were homogenized with pellet pestles, and RNA was isolated from three separate constructs using Trizol (Invitrogen) following standard protocols. RNA concentrations were obtained using a Nanodrop 2000 spectrophotometer. One μg of RNA was reverse-transcribed to cDNA using the Superscript First Strand Synthesis kit (Invitrogen). Real-time polymerase chain reaction (PCR) was performed on the cDNA using a Step One Plus system (Applied Biosystems) and the SYBR Green master mix (Applied Biosystems) using primers shown in Supplementary Table S1 (Supplementary Data are available online at www.liebertpub.com/tea). Relative expression levels compared to β-actin were determined using the $2^{-\Delta\Delta Ct}$ method. The reference condition chosen was PEGMA scaffolds containing no encapsulated HA at 4 days; all data were normalized to this condition.

In vivo *osteochondral defect model*

A rat osteochondral defect model was used to assess the potential of HA binding hydrogels to effect *in vivo* repair. All animal procedures were approved by the Johns Hopkins Animal Care and Use Committee (protocol #RA08A450). Male Sprague-Dawley rats (8 weeks) were anesthetized with 2%–3% Isoflurane using a tabletop anesthesia system (Vet-Equip). Hind limbs prepared using standard aseptic techniques, and an incision was made medial to the patellar tendon. The patella was displaced laterally to expose the articular surface of the femur. Round, 1-mm osteochondral defects were made in the patellar groove of the femur approximately 3 mm anterior to the ACL insertion point up to a depth of 1 mm. Defect depth was designed to approximate the depth used for microfracture procedures. Cartilage defect size was standardized through the use of a constant diameter drill bit to control defect diameter at 1 mm. Defect depth was controlled by drilling to a previously marked point on the bit.

Following defect creation, macromer solutions containing 10% PEGDA, 2% acryl-PEG-HABPep (or sHABPep), and 0.05% photoinitiator in PBS were placed into the defect site. Polymer solutions were photopolymerized by exposure to ultraviolet light for 5 min (365 nm, 5 mW/cm^2, Acticure 4000). During polymerization, hydrogels were partially mixed with blood and bone marrow that were present during the defect creation. Controls included scrambled peptide hydrogels and untreated defects. Incisions were closed and animals were allowed unrestricted movement for the duration of the study. A sample size of 6 knees was used for each material condition at each time point (4 days, 3 weeks, 6 weeks).

Histological evaluation of in vivo *repair*

At each time point, knees were dissected and excised. Implant areas were grossly imaged using a Zeiss Axiovert dissection microscope. Knees were decalcified and fixed for approximately a week in a solution of 10% formalin and 10% formic acid. Solution changes were performed every other day, at which point solutions were qualitatively assayed for calcium content using an oxalate precipitation test. Following a negative test, samples were immerse in increasing concentrations of a sucrose solution (up to 20% w/v) as a cryoprotectant, taking care to give adequate time for full tissue penetration. Then, samples were immersed in graded solutions of 20% sucrose and optimal cutting temperature (OCT) solution (Tissue-Tek), embedded in OCT, and frozen. Knees were cryosectioned at −20°C using a cryostat microtome (Leica) to section thicknesses of 7–10 μm. Sections were stained with Safranin-O and immunostained with type II collagen to visualize tissue morphology and repair.

Statistical analysis

Quantitative biochemical data were evaluated using multifactor analysis of variance to determine the significance of main factor effects to a significance level of 0.05. Multiple comparisons of individual condition means were carried out using the Tukey's honestly significant difference test. Statistical analysis was carried out in MATLAB (Mathworks).

Results

Incorporation of HA-binding elements into PEG hydrogels increases HA retention

HA release from PEG hydrogels depended on the initial HA loading dose. HA release from standard PEG hydrogels (without the HA interaction) was determined as a function of

initial HA loading. Various concentrations of HA (from 0–20 mg/mL) were loaded into control hydrogels (with no specific HA interaction) before polymerization, and the HA release profiles were measured by the carbazole assay to determine baseline HA release and any effects of nonspecific entanglement of HA with the crosslinked PEG gels (Fig. 1A). When high concentrations of HA were encapsulated in the PEG hydrogels, minimal HA was released, likely due to entanglement with the PEG network. When lower concentrations of HA (1 and 5 mg/mL) were encapsulated into the PEG hydrogels, the HA was quickly released. Percent HA release was significantly dependent on both HA loading and time ($p < 0.05$, Supplementary Fig. S1). Control hydrogels without HA did not yield any detectable levels of uronic acid using the carbazole assay. No evidence was found for covalent interactions between HA and the PEG network. Based on other studies with similar materials, it was assumed that high concentrations of HA can drive phase-separation processes that may create small pockets of higher concentration HA surrounded by pockets of higher concentration PEG, resulting in different diffusion kinetics.[20]

Incorporation of HA-binding peptides into PEG hydrogels modulated interactions, diffusion, and ultimately release of HA. PEG hydrogels conjugated with HA-binding or scrambled peptides were loaded with 5 mg/mL HA, the dose in which fast release was observed, and incubated in the presence and absence of hyaluronidase (Fig. 1B). The 5 mg/mL concentration of HA was selected for these release studies, since the HA is normally quickly released from PEG hydrogels. HA-interacting hydrogels released significantly less HA at equilibrium ($p < 0.05$) compared to hydrogels modified with scrambled peptide controls. With the addition of hyaluronidase, HA release did exhibit a small, but significant increase compared to incubation in PBS ($p < 0.05$, Supplementary Fig. S2).

Chondrogenic differentiation of MSCs in HA-binding PEG hydrogels

Cartilage formation by MSCs improved in HA-interacting scaffolds as evaluated by biochemical content, gene expression, and histological analysis. MSCs were encapsulated in HA-interacting scaffolds containing varying concentrations of HA and incubated in the chondrogenic medium for 6 weeks. The physical properties of these hydrogels varied depending on initial HA content and changed over the course of chondrogenic differentiation (Fig. 2A). At 4 days, the swelling ratio of HA-interacting and control hydrogels increased in an HA dose-dependent manner. However, as tissue developed over the culture period, the water content in the hydrogels varied. The swelling ratio depended significantly ($p < 0.05$) as a function of HA loading, and showed significant interactions between HA loading and time as well as hydrogel choice and time. Swelling did not directly depend on time or hydrogel choice (Supplementary Fig. S3).

HA-binding hydrogels increased cartilage production as determined by ECM production, cell number, and gene expression analysis. DNA content or cell number, in the control PEG hydrogels, decreased in an HA dose-dependent manner at all time points, but increased in HA-binding hydrogels containing increasing levels of exogenous HA at 4 days and 3 weeks. However, at later time points (6 weeks), DNA levels in the HA-interacting hydrogels decreased (Fig. 2B). Overall, DNA content depended significantly ($p < 0.05$) as a function of time and hydrogel choice. While HA loading was not a significant main effect, it demonstrated significant interactions with both time and hydrogel choice (Supplementary Fig. S4). GAG deposition in the hydrogels increased over time in all conditions (Fig. 2C, E). However, GAG levels decreased with higher exogenous HA loading in a dose-dependent manner for both control and HA-interacting hydrogels. HA-binding hydrogels produced significantly greater GAG levels than PEG and sHABPep controls, and hydrogels without any exogenous HA produced the greatest GAG matrix levels compared to all groups. GAG content depended significantly on all main factor effects ($p < 0.05$), and HA loading demonstrated significant interactions with both time and hydrogel choice (Supplementary Fig. S5). Total collagen deposition, represented by hydroxyproline content, in both HA-interacting and control hydrogels also increased over 6 weeks of chondrogenic culture (Fig. 2D, F).

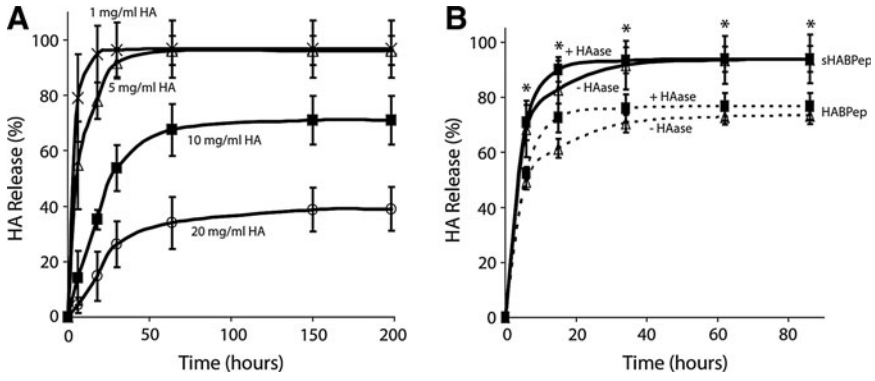

FIG. 1. Hyaluronic acid (HA)-interacting hydrogels increase retention of HA. **(A)** Release of HA from control noninteracting hydrogels was assessed at various HA loadings to determine the effects of nonspecific interactions between HA and poly(ethylene glycol) diacrylate. At steady state, HA loading concentrations of 1 mg/mL and 5 mg/mL were fully released from the hydrogel. **(B)** Specific interactions between HA and HABPep-functionalized hydrogels were assessed at 5 mg/mL HA loading. HABPep was shown to significantly decrease HA release at steady state (*denotes significance between HABPep and scrambled controls at each time point, $p < 0.05$). Addition of hyaluronidase increased the kinetics of release, but not the equilibrium behavior. HABPep, HA-binding peptide.

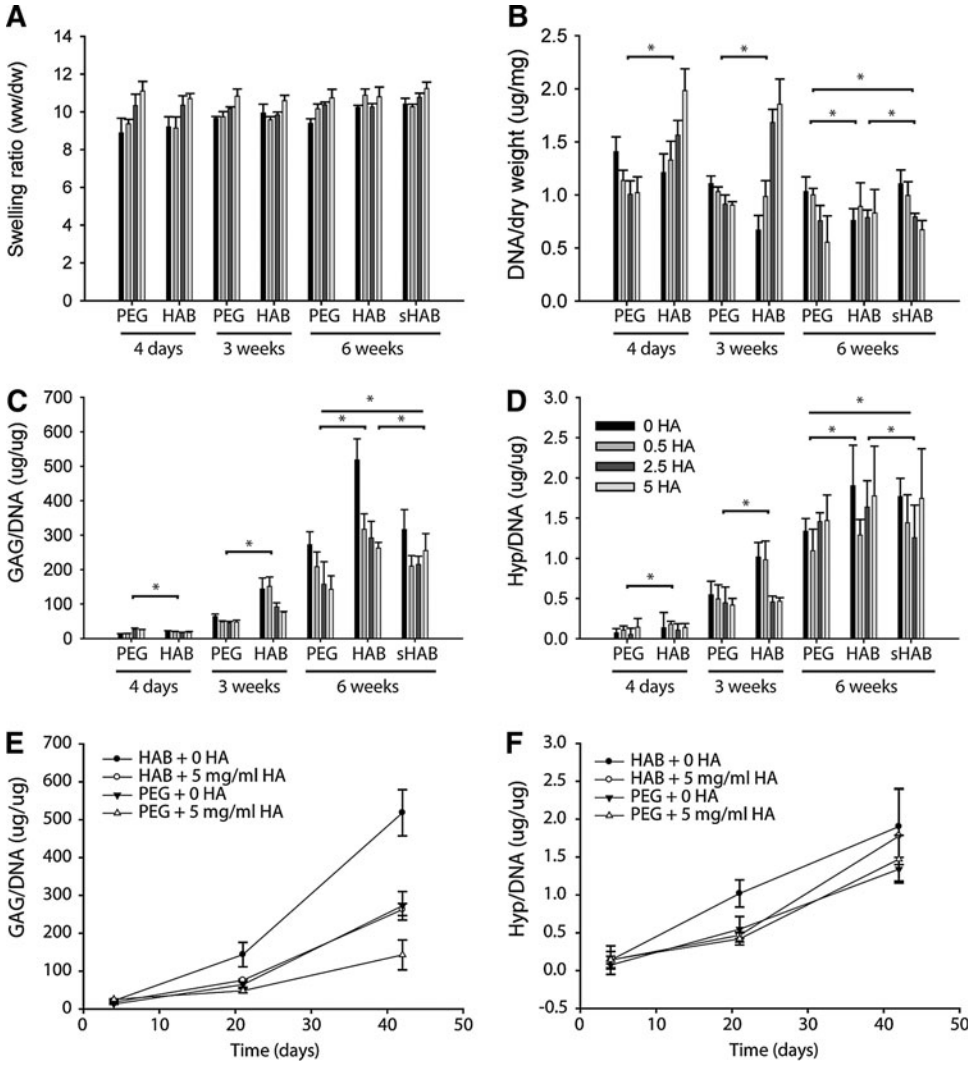

FIG. 2. HA-interacting hydrogels increased cartilage production by mesenchymal stem cells (MSCs). **(A)** Physical properties of PEG, HA-interacting (HAB), and scrambled peptide control (sHAB) hydrogels containing encapsulated MSCs varied with initial HA loading and culture time. Swelling was significantly dependent on HA loading ($p < 0.05$, see Fig. S3). **(B)** Cell number, as measured by DNA content, was initially highly dependent on scaffold type and HA loading, but differences decreased as scaffolds matured at 6 weeks. DNA was significantly dependent on hydrogel type and time, but not HA loading ($p < 0.05$, Fig. S4). **(C)** Glycosaminoglycan (GAG) content, normalized to DNA, increased with time for all scaffolds, with strong HA dose dependence at later weeks. GAG levels were significantly dependent on hydrogel type, HA loading, and time ($p < 0.05$). **(D)** Overall collagen production, as measured by hydroxyproline content normalized to DNA, increased over time for all scaffolds, but showed no specific trend across HA concentrations. Collagen content was significantly dependent on hydrogel type and time, but not HA loading ($p < 0.05$). GAG content **(E)** and collagen content **(F)** were plotted for representative HAB and PEG conditions over time. PEG, poly(ethylene glycol).

Hydroxyproline content depended significantly on hydrogel choice and time ($p < 0.05$), and HA loading interacted significantly with time (Supplementary Fig. S6). Overall, the ECM analysis in the hydrogels suggests that the HA-interacting hydrogels with little to no exogenous HA loading produced the greatest levels of new cartilage production.

Gene expression analysis of cartilage-related markers supported the chondrogenic differentiation of MSCs in the hydrogels (Fig. 3). Expression of *aggrecan*, an important protein in GAG structure and assembly, was largely unchanged at 4 days between HA-interacting and control hydrogels, though decreased with increasing HA loading. At 3 weeks, HA-interacting hydrogels demonstrated dramatically higher *aggrecan* expression than control hydrogels, peaking at 2.5 mg/mL exogenous HA loading. However, at 6 weeks, the control hydrogels expressed higher levels of *aggrecan* compared to HA-binding hydrogels, with exogenous HA producing a dose-dependent decrease in expression. In the case of *type II collagen*, no significant differences were observed between HA-binding hydrogels and controls at 4 days and 3 weeks, while intermediate HA loading of HA-binding hydrogels exhibited a significant upregulation at 6 weeks. Levels of *type I collagen* expression were also upregulated in HA-binding hydrogels, but to a much lesser degree than the upregulation of *type II collagen* and *aggrecan*.

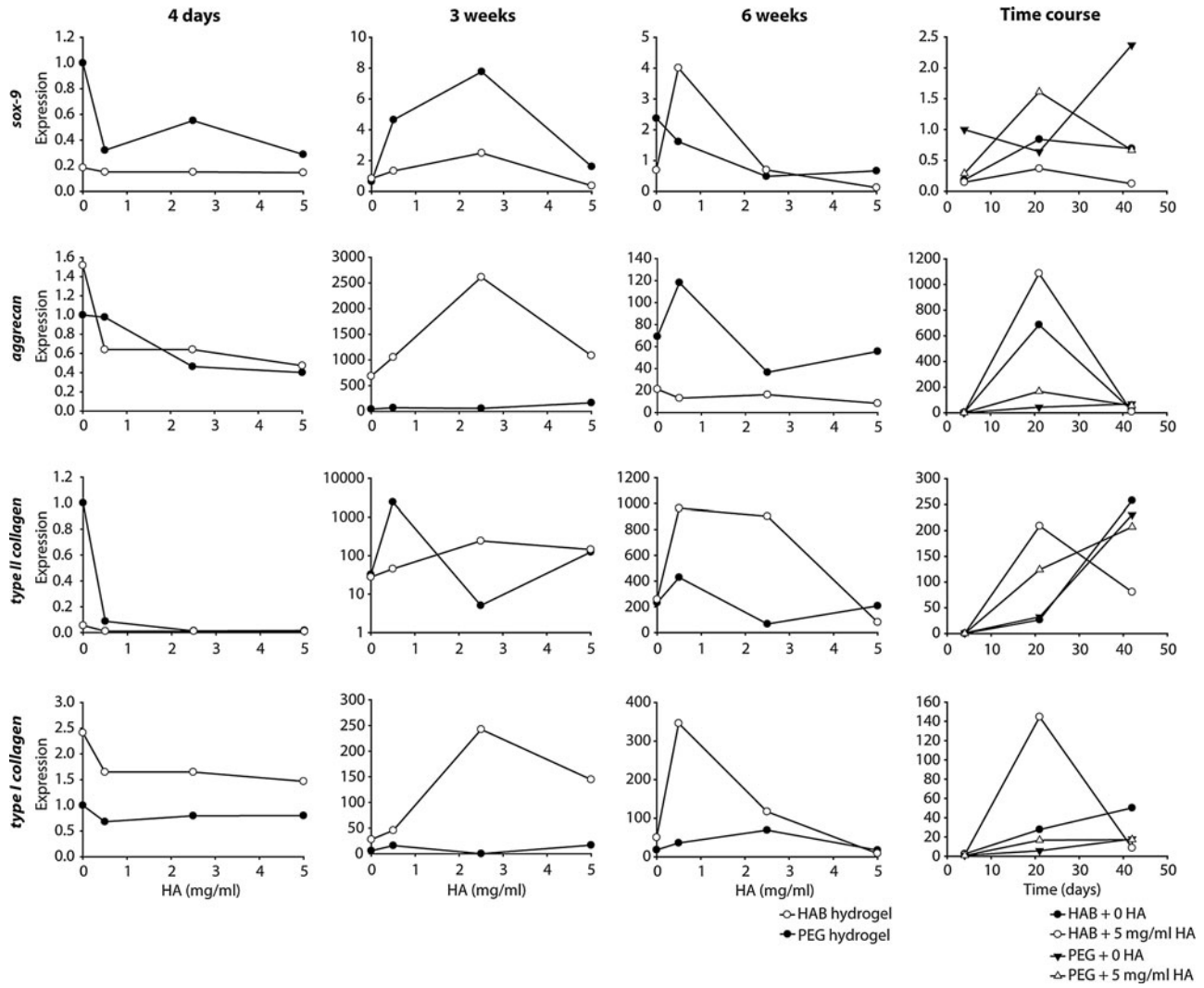

FIG. 3. Gene expression demonstrates chondrogenic differentiation of MSCs in HA-interacting hydrogels. *Sox-9, aggrecan, type II collagen,* and *type I collagen* expression were analyzed for all hydrogel conditions. All expression levels were normalized to individual *β-actin* levels and observed expression for PEG scaffolds containing no HA at 4 days. HA-interacting hydrogels increased *aggrecan* production at 3 weeks and *type II collagen* production at 6 weeks.

Histological analysis supports the biochemical results that the HA-interactive scaffolds produce greater levels of cartilage tissue components after 6 weeks. Safranin O staining of harvested constructs (Fig. 4) exhibited a substantial increase in GAG deposition in HA-interacting hydrogels at 3 weeks compared to controls. In addition to the concentrated GAG staining in the pericellular region, HA-binding hydrogels contained higher staining in the intercellular regions of the hydrogel material, suggesting the scaffold has retained cell-secreted proteoglycans by binding to the HA core. The differences in staining were less pronounced at 6 weeks between the groups, though HA-interactive scaffolds still had more intense staining. Safranin O staining was also a function of initial HA loading, with more intense staining observed for lower loading for both control and HA-binding scaffolds, similar to the quantified ECM results. Type II collagen immunostaining of control hydrogels at 3 weeks was slightly more intense than HA-interactive scaffolds. However, after 6 weeks, HA-binding PEG hydrogels produced significantly greater Type II collagen staining compared to PEG controls.

Repair of osteochondral defects in vivo *with hydrogels*

Implantation of HA-interactive PEG hydrogels increased cartilage tissue production in osteochondral defects created on the rat femoral condyle compared to control hydrogels and untreated defects. Acellular scaffolds were implanted in the defects to avoid the challenge of delivering exogenous cells. The implanted scaffolds were able to integrate with the surrounding tissue, and gross images of harvested knees after 4 days following implantation demonstrated that hydrogels remained in the defects and achieved good material-tissue integration (Supplementary Fig. S7).

Implantation of HA-interactive hydrogels in osteochondral defects resulted in a more robust cartilage tissue repair compared to control hydrogels and untreated defects (Fig. 5). After 4 days, discrete hydrogel material was clearly visible in

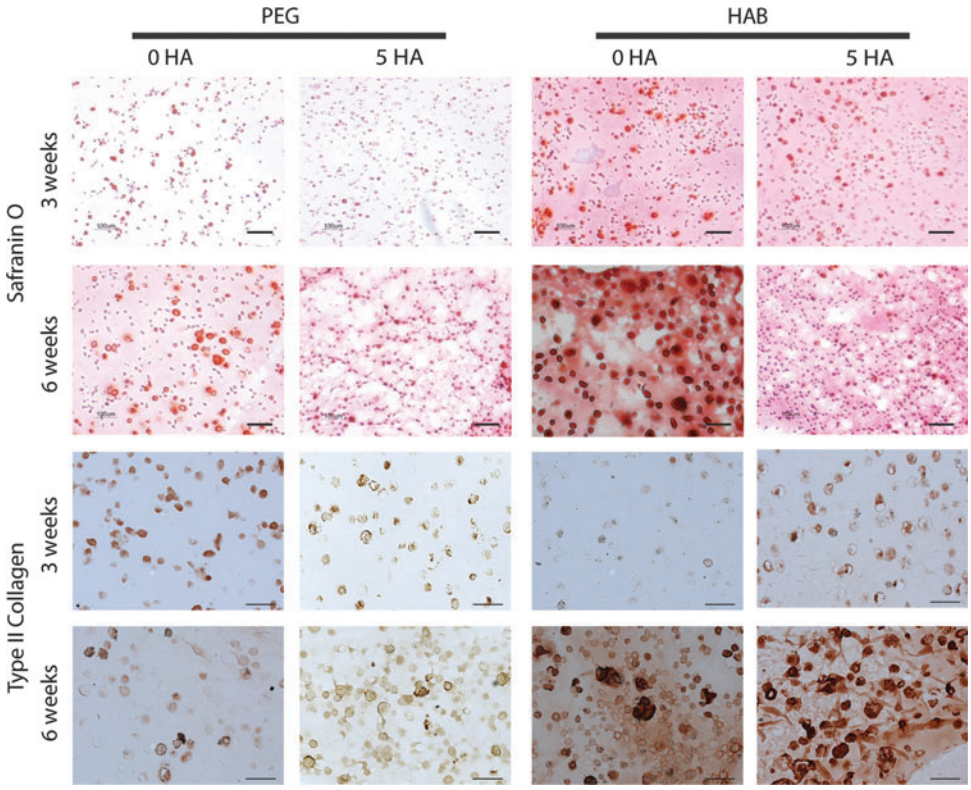

FIG. 4. HA-interactive scaffolds accumulate more cartilage matrix components at 6 weeks. Safranin O staining of HA-interactive scaffolds and PEG scaffolds across 6 weeks demonstrates increased GAG deposition in HA-interactive scaffolds. Staining is highest for low HA loadings. Immunohistochemical staining for Type II collagen indicated initially higher staining for PEG controls at 3 weeks, but substantially higher staining for HA-interactive scaffolds at 6 weeks. Bar = 100 μm.

the HA-interactive and scrambled peptide control conditions, while the untreated defects were filled with a clot, cells, and tissue debris. Both HA-binding and control hydrogels appeared to be well-integrated into the surrounding tissue with cell infiltration present at the margins of the implants. Scrambled peptide controls exhibited a significantly stronger tissue response with more cells at the implant edge. After 3 weeks, the implant material was still evident for both HA-binding and control hydrogels, though the surrounding tissue response had mostly subsided and the underlying subchondral bone was undergoing repair.

Although there was as yet no clear, differentiated cartilage-like repair tissue visible, there were some early signs of repair at the margins of the defect that did not stain positive

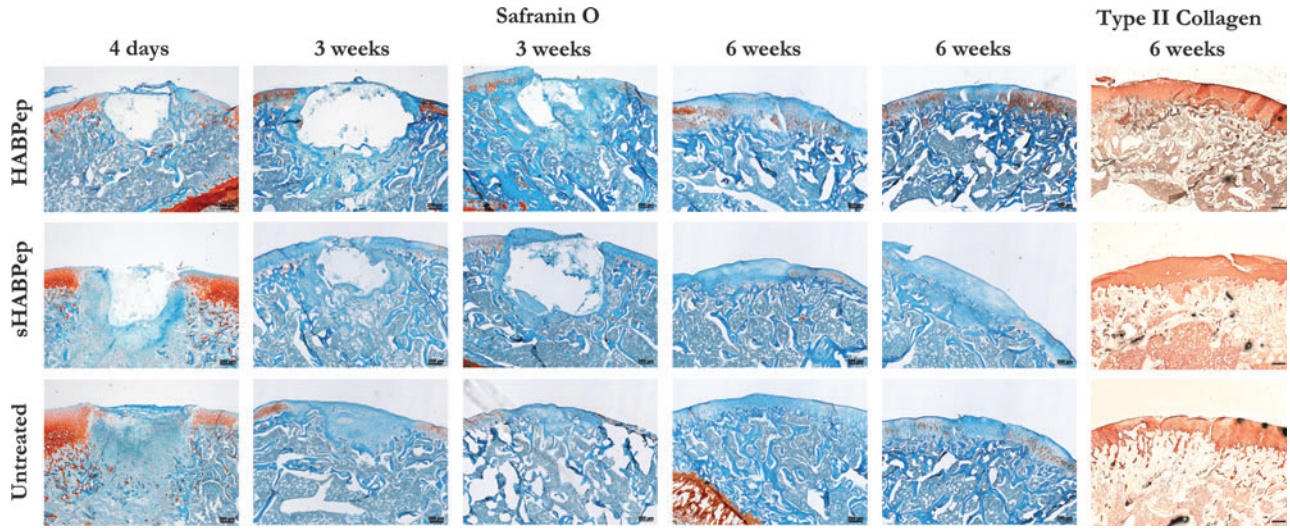

FIG. 5. HA-interactive scaffolds assist in the repair of rat osteochondral defects *in vivo*. Safranin O staining of osteochondral defects in representative rat knees demonstrated that HA-interactive hydrogels produced more GAG-positive repair tissue than scrambled peptide controls (sHABPep) or untreated defects. In addition, tissue adjacent to the defects treated with HA-interactive scaffolds contained more GAGs than controls. Representative Safranin O sections are shown for two separate animals at 3 and 6 weeks postimplantation for comparison. Type II collagen immunostaining did not show substantial differences in collagen content. Bar = 200 μm.

for Safranin O. Untreated defect controls exhibited a smaller defect depth, but no visible Safranin O-positive cartilage repair. At 6 weeks, implant material was entirely absent and replaced with varying levels of repair tissue. Neither HA-binding nor scrambled peptide control hydrogels caused a complete regeneration of healthy cartilage at this time point, but HA binding hydrogels produced a greater volume of repair tissue with stronger Safranin O staining compared to controls, though still weaker than healthy tissue. Untreated defects showed a well-integrated repair tissue with minimal Safranin O staining, indicative of the expected fibrocartilagenous repair.

The presence of the HA-interactive hydrogels in the osteochondral defects also had an impact on the ECM of the cartilage surrounding the defect. At 3 weeks, all knees exhibited reduced Safranin O staining for GAGs on articular cartilage surrounding the defect and in the joint space compared to day 4 staining and untreated controls. At 6 weeks, Safranin O staining of cartilage outside the defect area was further reduced, suggesting the presence of a discrete osteochondral defect also caused degenerative joint changes. However, joints containing defects treated with HA-interactive scaffolds exhibited greater proteoglycan staining, indicating reduced cartilage degeneration. Overall, these results indicate that HA-binding hydrogels produced an improvement in the repair of osteochondral defects and the maintenance of cartilage tissue surrounding the defect.

Discussion

The goal of this research was to develop a novel HA-binding hydrogel that would interact noncovalently with HA. While the HA-interacting scaffold was able to modulate the release of HA doped into the hydrogel, the potential scaffold interaction with cell-secreted or local ECM-derived HA may also influence tissue remodeling and regeneration. Noncovalent binding of a critical matrix building block may allow a more efficient matrix assembly when required during the tissue development process. Since HA is a critical matrix component or the building block of the ECM in many tissues, providing a scaffold that can reversibly bind the molecule could have widespread application in regeneration.

The role of HA in the development of cartilage has been well studied, but its application to tissue engineering has yielded varying results. In development, HA plays a critical role during mesenchymal condensation that leads to cartilage formation. Early in this process, the limb mesenchyme is composed of dispersed cells throughout an ECM that contains significant quantities of HA. Upon initiation of condensation, mesenchymal cells aggregate, hyaluronidases are upregulated, and HA concentrations drop. It is believed that HA helps mediate cell aggregation as an intercell bridge through multivalent binding to HA receptors, notably CD44. High concentrations of HA can saturate the cell receptors without the attendant bridging effects, and thus inhibit or slow mesenchymal condensation. After condensation, HA synthesis is again upregulated as the cells differentiate toward a functional cartilage tissue.[21] This is supported by research showing that addition of HA inhibits chick limb bud morphogenesis and later cartilage formation, and that HAase activity is spatially and temporally regulated in a very precise manner during limb bud development.[22–24]

The connection between embryological roles of HA and its uses in tissue engineering are less understood. Previous studies in our laboratory show agreement that HA encapsulation in synthetic hydrogels does not produce a strong chondrogenic response *in vitro*, but may in fact help osteogenesis.[7] Other studies from Burdick and coworkers, however, who have used an HA-based hydrogel with a variety of cell types, indicate that while modified HA hydrogels are supportive of embryonic stem cell self-renewal, they are supportive of differentiation and tissue formation when used with MSCs and chondrocytes. These results suggest that less differentiated cell types respond to HA as a proliferative and self-renewal signal, while partially differentiated cells respond to HA by enhancing chondrogenesis.[6,25,26] In the present studies, HA-interactive scaffolds (with little exogenous HA) significantly improved cartilage tissue formation *in vitro*. However, hydrogels containing exogenous HA increased cell number at early time points, evidencing either an increase in proliferation or an improvement in cell viability. We speculate that the observed high levels of matrix synthesis in HA-interactive scaffolds at later time points may act as a signal that there are too many matrix-producing cells in a tissue, resulting in a lower cell number at 6 weeks. These results of HA improving cell survival or proliferation at early time points, yet inhibiting matrix production at later time points, highlight the importance of controlling the temporal presentation of extracellular signals during cell differentiation.

In addition to the overall improvement in chondrogenesis observed with the HA-interactive scaffolds, the temporal dynamics of tissue formation more closely resembled the embryologic development of cartilage tissue. Histological staining and gene expression both confirmed early increases in GAG deposition and aggrecan synthesis, with lower Type II collagen production compared to controls. However by 6 weeks, Type II collagen expression and deposition significantly increased compared to controls. These data correlate with observations during limb embryogenesis, where GAG deposition precedes Type II collagen synthesis.[27] Previous studies have suggested that pericellular GAG molecules can aid in the organization and deposition of Type II collagen during chondrogenesis.[28] This may explain the marked increase in Type II collagen deposition by 6 weeks compared to control materials. The cell-secreted proteoglycans, bound to the HA-interactive scaffold through their HA cores, may aid in the deposition and organization of Type II collagen.

After *in vitro* testing, the biomaterial formulation that produced the greatest cartilage, the HA-binding hydrogels with no HA loading, was selected for translation to an *in vivo* study to evaluate repair of osteochondral defects. The goal of the *in vivo* studies was to provide a material that would direct the differentiation of endogenous repair cells. While cells can be added to the biomaterial before implantation, clinical translation potential is increased if an off-the-shelf material is available to combine with surgical procedures. Defects treated with the HA-interactive scaffolds produced more organized repair tissue that stained more strongly for Safranin O compared to untreated defects, though still below that of healthy cartilage. Repair tissue was still clearly distinguishable from the surrounding cartilage after 6 weeks, and in some cases active remodeling was still present. Additional time, up to 9 or 12 weeks, may provide the

opportunity for more remodeling and ultimately more complete repair.

An unexpected observation in joint studies was the impact of the HA-interactive scaffolds on reducing degeneration of tissue surrounding the defects. The cartilage tissue surrounding the osteochondral defects demonstrated degenerative changes, such as reduced proteoglycan content, over the course of the experiment. The potential of cartilage defects to lead to generalized degenerative changes in the joint is a well-known phenomenon that is the basis of the clinical desire to treat cartilage defects to prevent post-traumatic osteoarthritis. Implanting defects with the HA-interactive scaffolds reduced the decrease in Safranin O staining in the surrounding tissues. There are a number of potential physical and biological mechanisms for this observation. HA bound to the surface of the hydrogel may enhance lubrication, reducing friction at the defect and surrounding cartilage surface. HA also has anti-inflammatory properties, which may improve overall joint homeostasis as the defect is undergoing repair.

In conclusion, HA-interacting hydrogels can improve cartilage tissue formation *in vitro* and *in vivo*. The results indicated that early presentation of HA to MSCs results in a more proliferative phenotype, while later presentation of cell-secreted HA results in a more chondrogenic phenotype than controls. The use of a smart, matrix-interacting material allowed for the recapitulation of events during limb bud development with temporal increases in proteoglycan followed by Type II collagen production. The HA-binding hydrogels improved repair of osteochondral defects, and were able to reduce degeneration in cartilage surrounding the defects. Matrix-interactive materials are a promising candidate as biomaterials for applications, including repair and regeneration due to their high degree of control, the natural presentation of native matrix molecules, and their dynamic, cell-directed presentation of ECM components.

Acknowledgments

This investigation was supported by the National Institutes of Health under Ruth L. Kirschstein National Research Service Award #AG328232. We gratefully acknowledge Johns Hopkins A.B. Mass Spectrometry/Proteomic Facility for providing the MALDI-TOF spectrometer and the Johns Hopkins Department of Chemistry Instrumentation Facility for providing the peptide synthesizer.

Disclosure Statement

No competing financial interests exist.

References

1. Volpi, N., Schiller, J., Stern, R., and Soltes, L. Role, metabolism, chemical modifications and applications of hyaluronan. Curr Med Chem **16,** 1718, 2009.
2. Chung, C., Beecham, M., Mauck, R.L., and Burdick, J.A. The influence of degradation characteristics of hyaluronic acid hydrogels on *in vitro* neocartilage formation by mesenchymal stem cells. Biomaterials **30,** 4287, 2009.
3. Shu, X.Z., Ahmad, S., Liu, Y., and Prestwich, G.D. Synthesis and evaluation of injectable, *in situ* crosslinkable synthetic extracellular matrices for tissue engineering. J Biomed Mater Res Part A **79,** 902, 2006.
4. Park, Y.D., Tirelli, N., and Hubbell, J.A. Photopolymerized hyaluronic acid-based hydrogels and interpenetrating networks. Biomaterials **24,** 893, 2003.
5. Liu, Y., Shu, X.Z., and Prestwich, G.D. Osteochondral defect repair with autologous bone marrow-derived mesenchymal stem cells in an injectable, *in situ*, cross-linked synthetic extracellular matrix. Tissue Eng **12,** 3405, 2006.
6. Gerecht, S., Burdick, J.A., Ferreira, L.S., Townsend, S.A., Langer, R., and Vunjak-Novakovic, G. Hyaluronic acid hydrogel for controlled self-renewal and differentiation of human embryonic stem cells. Proc Natl Acad Sci U S A **104,** 11298, 2007.
7. Hwang, N.S., Varghese, S., Li, H., and Elisseeff, J. Regulation of osteogenic and chondrogenic differentiation of mesenchymal stem cells in PEG-ECM hydrogels. Cell Tissue Res **344,** 499, 2011.
8. Mano, J.F., Silva, G.A., Azevedo, H.S., Malafaya, P.B., Sousa, R.A., Silva, S.S., *et al.* Natural origin biodegradable systems in tissue engineering and regenerative medicine: present status and some moving trends. J R Soc Interface **4,** 999, 2007.
9. Gunatillake, P., Mayadunne, R., and Adhikari, R. Recent developments in biodegradable synthetic polymers. Biotechnol Annu Rev **12,** 301, 2006.
10. Ifkovits, J.L., and Burdick, J.A. Review: photopolymerizable and degradable biomaterials for tissue engineering applications. Tissue Eng **13,** 2369, 2007.
11. Hern, D.L., and Hubbell, J.A. Incorporation of adhesion peptides into nonadhesive hydrogels useful for tissue resurfacing. J Biomed Mater Res **39,** 266, 1998.
12. Zustiak, S.P., Durbal, R., and Leach, J.B. Influence of cell-adhesive peptide ligands on poly(ethylene glycol) hydrogel physical, mechanical and transport properties. Acta Biomaterialia **6,** 3404, 2010.
13. Lee, H.J., Yu, C., Chansakul, T., Hwang, N.S., Varghese, S., Yu, S.M., *et al.* Enhanced chondrogenesis of mesenchymal stem cells in collagen mimetic peptide-mediated microenvironment. Tissue Eng Part A **14,** 1843, 2008.
14. Salinas, C.N., and Anseth, K.S. The enhancement of chondrogenic differentiation of human mesenchymal stem cells by enzymatically regulated RGD functionalities. Biomaterials **29,** 2370, 2008.
15. Martino, M.M., Tortelli, F., Mochizuki, M., Traub, S., Ben-David, D., Kuhn, G.A., *et al.* Engineering the growth factor microenvironment with fibronectin domains to promote wound and bone tissue healing. Sci Transl Med **3,** 100ra89. 2011.
16. Mummert, M.E., Mohamadzadeh, M., Mummert, D.I., Mizumoto, N., and Takashima, A. Development of a peptide inhibitor of hyaluronan-mediated leukocyte trafficking. J Exp Med **192,** 769, 2000.
17. Zmolik, J.M., and Mummert, M.E. Pep-1 as a novel probe for the *in situ* detection of hyaluronan. J Histochem Cytochem **53,** 745, 2005.
18. Bitter, T., and Muir, H.M. A modified uronic acid carbazole reaction. Anal Biochem **4,** 330, 1962.
19. Williams, C.G., Kim, T.K., Taboas, A., Malik, A., Manson, P., and Elisseeff, J. *In vitro* chondrogenesis of bone marrow-derived mesenchymal stem cells in a photopolymerizing hydrogel. Tissue Eng **9,** 679, 2003.
20. Dong, Y., Hassan, W., Zheng, Y., Saeed, A.O., Cao, H., Tai, H., *et al.* Thermoresponsive hyperbranched copolymer with multi acrylate functionality for *in situ* cross-linkable hyaluronic acid composite semi-IPN hydrogel. J Mater Sci Mater Med **23,** 25, 2012.

21. Maleski, M.P., and Knudson, C.B. Hyaluronan-mediated aggregation of limb bud mesenchyme and mesenchymal condensation during chondrogenesis. Exp Cell Res **225,** 55, 1996.
22. Toole, B.P., Jackson, G., and Gross, J. Hyaluronate in morphogenesis: inhibition of chondrogenesis *in vitro*. Proc Natl Acad Sci U S A **69,** 1384, 1972.
23. Kulyk, W.M., and Kosher, R.A. Temporal and spatial analysis of hyaluronidase activity during development of the embryonic chick limb bud. Dev Biol **120,** 535, 1987.
24. Li, Y., Toole, B.P., Dealy, C.N., and Kosher, R.A. Hyaluronan in limb morphogenesis. Dev Biol **305,** 411, 2007.
25. Chung, C., and Burdick, J.A. Influence of three-dimensional hyaluronic acid microenvironments on mesenchymal stem cell chondrogenesis. Tissue Eng Part A **15,** 243, 2009.
26. Chung, C., Mesa, J., Randolph, M.A., Yaremchuk, M., and Burdick, J.A. Influence of gel properties on neocartilage formation by auricular chondrocytes photoencapsulated in hyaluronic acid networks. J Biomed Mater Res Part A **77,** 518, 2006.
27. Módis, L. Organization of the Extracellular Matrix: A Polarization Microscopic Approach. Boca Raton, FL: CRC Press, 1990.
28. Graff, R.D., Kelley, S.S., and Lee, G.M. Role of pericellular matrix in development of a mechanically functional neocartilage. Biotechnol Bioeng **82,** 457, 2003.

Address correspondence to:
Jennifer H. Elisseeff, Ph.D.
Department of Biomedical Engineering
Johns Hopkins University
Smith Building Rm. 5033
400 N. Broadway
Baltimore, MD 21231

E-mail: jhe@jhu.edu

Received: December 15, 2011
Accepted: June 22, 2012
Online Publication Date: August 14, 2012